

# Cross-view Action Recognition Understanding From Exocentric to Egocentric Perspective

Thanh-Dat Truong, Khoa Luu  
Computer Vision and Image Understanding Lab  
University of Arkansas, Fayetteville, AR, 72701  
{tt032, khoaluu}@uark.edu

## Abstract

Understanding action recognition in egocentric videos has emerged as a vital research topic with numerous practical applications. With the limitation in the scale of egocentric data collection, learning robust deep learning-based action recognition models remains difficult. Transferring knowledge learned from the large-scale exocentric data to the egocentric data is challenging due to the difference in videos across views. Our work introduces a novel cross-view learning approach to action recognition (CVAR) that effectively transfers knowledge from the exocentric to the egocentric view. First, we introduce a novel geometric-based constraint into the self-attention mechanism in Transformer based on analyzing the camera positions between two views. Then, we propose a new cross-view self-attention loss learned on unpaired cross-view data to enforce the self-attention mechanism learning to transfer knowledge across views. Finally, to further improve the performance of our cross-view learning approach, we present the metrics to measure the correlations in videos and attention maps effectively. Experimental results on standard egocentric action recognition benchmarks, i.e., Charades-Ego, EPIC-Kitchens-55, and EPIC-Kitchens-100, have shown our approach’s effectiveness and state-of-the-art performance.

## 1. Introduction

Analyzing first-view videos, i.e., egocentric videos, captured by wearable cameras has become an active research topic in recent years. With the recent development of virtual and augmented reality technologies, this topic has gained more attention in the research communities due to the enormous interest in analyzing human behaviors from the first-view perspective. Many tasks have been currently explored in the egocentric video data that provide many practical applications, e.g., action recognition [48, 56, 49, 46, 51], action detection [15, 85, 84, 38, 76], action anticipation [30, 51, 54], etc. In comparison with third-view video data, i.e., exocentric videos, egocentric videos provide new, dis-

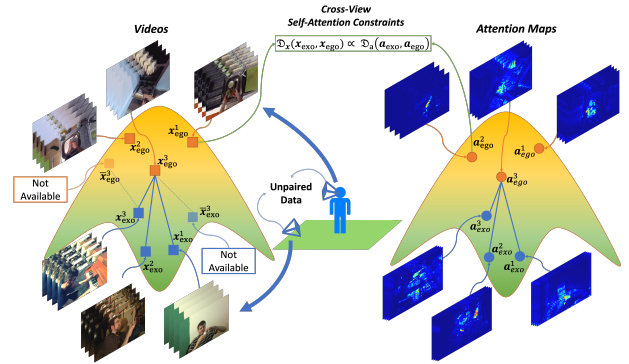


Figure 1. **The Cross-view Self-attention Constraints.** Although under the setting of cross-view unpaired data where the corresponding video and its attention in the opposite view are inaccessible, our cross-view self-attention loss is proven to impose the cross-view constraints via unpaired samples based on the geometric properties between two camera positions.

tinct viewpoints of surrounding scenes and actions driven by the camera position holding on the observer.

The properties of egocentric videos also bring new challenges to video analysis tasks. One of the main issues is the scale of datasets. It is well known that learning robust video models, e.g., action recognition models, usually requires a large amount of video data [56, 49, 51]. For example, the third-view action models are learned on the large-scale Kinetics-700 [11] data that consists of 650K videos over 700 classes. Meanwhile, the scale of egocentric video data is relatively small compared to third-view datasets, e.g., EPIC Kitchens [15] only consists of 90K clips or Charades-Ego [72] includes 68K clips of 157 classes. In addition, the egocentric video data lack variation, e.g., videos only in kitchens [15] or daily indoor activities [72]. These problems pose a considerable challenge for learning robust video models on the first-view data.

Many prior works [51, 26] have improved the performance of action recognition models by adopting the pre-trained model on large-scale third-view datasets and fine-tuning it on the first-view dataset. However, these meth-

ods often ignore the unique characteristics of egocentric videos. Thus, they could meet the unaligned domain problems. Another method [48] has tried to alleviate this domain mismatch problem by introducing several additional egocentric tasks during the pre-training phase on the third-view datasets. However, this approach requires the labels of egocentric tasks on third-view data or relies on the off-the-shelf specific-task models. Domain adaptation methods [48, 33, 71] have also been utilized to transfer the knowledge from the third-view to first-view data. Nevertheless, these methods still need to model the camera-view changes during the adaptation phase.

With the recent success of Vision Transformer, the self-attention mechanism is fundamental to building an efficient action recognition model. Still, fewer prior works have focused on leveraging self-attention to model action recognition from the third-view to first-view data. Moreover, modeling the change in camera positions across views is also one of the primary factors in sufficiently developing a learning approach from the exocentric to egocentric view. Therefore, taking these characteristics into consideration, we introduce a novel cross-view learning approach to model the self-attention mechanism to effectively transfer the knowledge learned on third-view to first-view data. Our proposed approach first considers the geometric correlation between two camera views. Then, the cross-view geometric correlation constraint is further embedded into the self-attention mechanism so that the model can generalize well from the exocentric to the egocentric domain. Fig. 1 illustrates the cross-view self-attention constraint.

**Contributions of this Work:** This work introduces a novel **Cross-View** learning approach to **Action Recognition** (CVAR) via effectively transferring knowledge from the exocentric video domain to the egocentric one. By analyzing the role of the self-attention mechanism and the change of camera position across views, we introduce a new geometric cross-view constraint for correlation between videos and attention maps. Then, from the proposed cross-view restriction, we present a novel cross-view self-attention loss that models the cross-view learning into the self-attention mechanism. Our proposed loss allows the Transformer-based model to adapt knowledge and generalize from the third-view to first-view video data. The cross-view correlations of videos and attention maps are further enhanced using the deep metric and the Jensen-Shannon divergence metric, respectively, that capture deep semantic information. Our experimental results on the standard egocentric benchmark, i.e., Charades-Ego, EPIC-Kitchens-55, and EPIC-Kitchens-100, have illustrated the effectiveness of our proposed method and achieved state-of-the-art (SOTA) results.

## 2. Related Work

**Video Action Recognition** Many large-scale third-view datasets have been introduced for action recognition tasks, e.g., Kinetics [44, 10, 11], Something-Something V2 [34], Sport1M [42], AVA [36], etc. Many deep learning approaches [12, 26, 86, 50, 5, 56, 24, 49] have been introduced and achieved remarkable achievements. The early deep learning approaches [42, 19] have utilized the 2D Convolutional Neural Networks (CNNs) [37, 74, 78] to extract the deep spatial representation followed by using Recurrent Neural Networks (RNNs) [39] to learn the temporal information from these extracted spatial features. Some later approaches have improved the temporal learning capability by introducing the two-stream networks [73, 29, 27, 28, 86] using both RGB video inputs and optical flows for motion modeling. Later, the 3D CNN-based approaches [81] and their variants [12, 93] have been introduced, i.e., several (2+1)D CNN architectures have been proposed [82, 26, 25, 90]. Meanwhile, other approaches have used pseudo-3D CNNs built based on 2D CNNs [50, 63]. In addition, to better capture the long-range temporal dependencies among video frames, the non-local operation has also been introduced [88]. SlowFast [26] proposes a dual-path network to learn spatiotemporal information at two different temporal rates. X3D [25] progressively expands the networks to search for an optimal network for action recognition.

**Vision Transformer** [20, 5, 56, 24, 49, 8, 83] has become a dominant backbone in various tasks due to its outstanding performance. The early success of Video Vision Transformer (ViViT) [5] has shown its promising capability in handling spatial-temporal tokens in action recognition. Then, many variants [56, 8, 24, 49, 83] of ViViT has been introduced to not only improve the accuracy but also reduce the computational cost. [9] presented a space-time mixing attention mechanism to reduce the complexity of the self-attention layers. TimeSFormer [8] introduced divided spatial and temporal attention to reduce the computational overhead. Then, it is further improved by using the directed attention mechanism [83]. Then, [24] proposed a Multi-scale Vision Transformer (MViT) by using multiscale feature hierarchies. Then, MViT-V2 [49] improves the performance of MViT by incorporating decomposed relative positional embeddings and residual pooling connections. Swin Video Transformer [56] has achieved state-of-the-art performance in action recognition by using shifted windows to limit the self-attention computational cost to local windows and also allow learning attention across windows.

**Egocentric Video Analysis** Apart from third-view videos, egocentric videos provide distinguished viewpoints that pose several challenges in action recognition. Many datasets have been introduced to support the egocentric video analysis tasks, e.g., Charades-Ego [72], EPIC Kitchens [16, 15], Ego4D [35], EgoClip [51], HOI4D [55].

These datasets provide several standard egocentric benchmarks, e.g., action recognition [72, 16, 35], action anticipation [35, 15], action detection [15], video-text retrieval [35, 51]. Many methods have been proposed for egocentric action recognition, including Multi-stream Networks [58, 47, 45, 87], RNNs [32, 31, 77], 3D CNNs [62, 57], Graph Neural Networks [60]. Despite the difference in network designs, these prior works are usually pre-trained on the large-scale third-view datasets before fine-tuning them on the first-view dataset. However, there is a significant difference between the first-view and third-view datasets. Thus, a direct fine-tuning approach without consideration of modeling view changes could result in less efficiency. Many methods have improved the performance of the action recognition models by using additional egocentric cues or tasks, including gaze and motor attention [59, 47, 53], object detection [30, 7, 17, 89], hand interactions [79, 67, 41]. Ego-Exo [48] presented an approach by introducing the auxiliary egocentric tasks i.e., ego-score, object-score, and interaction map predictions, into the pre-training phase on the third-view dataset. However, these methods usually require the labels of auxiliary egocentric tasks on the third-view datasets or rely on pseudo labels produced by the off-the-shelf pre-trained models on egocentric tasks.

**Cross-view Video Learning** The cross-view learning approaches have been exploited and proposed for several tasks, e.g., geo-localization [94, 80, 70, 69], semantic segmentation [14, 66, 18]. Meanwhile, in video understanding tasks, several prior methods have alleviated the cross-view gap between exocentric and egocentric domains by using domain adaptation [33, 13], learning viewpoint-invariant [75, 71, 2, 68], or learning joint embedding [91, 1, 3, 4, 92]. Other works utilized generative models to synthesize the other viewpoints from a given image/video [22, 64, 65, 52]. However, these methods often require either a pair of data of both first and third views to learn the joint embedding or a share label domain when using domain adaptation.

### 3. Cross-view Learning in Action Recognition

Let  $\mathbf{x}_{exo} \in \mathbb{R}^{T \times H \times W \times 3}$  be a third-view (exocentric) video and  $\mathbf{y}_{exo} \in \mathcal{Y}_{exo}$  be its corresponding ground-truth class,  $\mathcal{Y}_{exo}$  is the set of classes in the exocentric dataset. Similarly,  $\mathbf{x}_{ego} \in \mathbb{R}^{T \times H \times W \times 3}$  be a first-view (egocentric) video and  $\mathbf{y}_{ego} \in \mathcal{Y}_{ego}$  be its corresponding ground-truth class,  $\mathcal{Y}_{ego}$  is the set of classes in the egocentric dataset. Let  $F : \mathbb{R}^{T \times H \times W \times 3} \rightarrow \mathbb{R}^D$  be the backbone network that maps a video into the deep representation,  $C_{exo}$  and  $C_{ego}$  are the classifier of exocentric and egocentric videos that predict the class probability from the deep representation. Then, the basic learning approach to learning the action model from the exocentric to the egocentric view can

be formulated as a supervised objective, as in Eqn. (1).

$$\arg \min_{\theta_F, \theta_{C_{exo}}, \theta_{C_{ego}}} [\mathbb{E}_{\mathbf{x}_{exo}, \mathbf{y}_{exo}} \mathcal{L}_{ce}(C_{exo}(F(\mathbf{x}_{exo})), \mathbf{y}_{exo}) + \mathbb{E}_{\mathbf{x}_{ego}, \mathbf{y}_{ego}} \mathcal{L}_{ce}(C_{ego}(F(\mathbf{x}_{ego})), \mathbf{y}_{ego})] \quad (1)$$

where  $\theta_F, \theta_{C_{exo}}, \theta_{C_{ego}}$  are the network parameters,  $\mathcal{L}_{ce}$  is the supervised loss (i.e., cross-entropy loss). Several prior approaches [48, 71] have adopted this learning approach to learn a cross-view action recognition model. Then, other prior methods have further improved the performance of models by using a large pretrained model [26, 56], domain adaptation [33], learning a joint embedding between two views [71], learning auxiliary egocentric tasks [48].

Although these prior approaches [26, 48, 56, 49] showed their potential in improving performance, they have not effectively addressed the problem of cross-view learning. In particular, domain adaptation methods [33] are often employed in the context of environment changes (e.g., simulation to real data), and the camera views are assumed on the same position (either third view or first view). However, there is a huge difference in videos between the third view and the first view. Thus, domain adaptation is considered less effective in the cross-view setting. Meanwhile, fine-tuning the first-view action model on the large pre-trained models [26, 56] usually relies on the deep representation learned from the large-scale third-view data. However, these deep representations do not have any guarantee mechanism well generalized in the first-view video. Also, learning the joint embedding or auxiliary egocentric tasks [48] suffer a similar problem due to their design of learning approaches without the consideration of camera changes. In addition, it requires a pair of views of video data during training. Therefore, to effectively learn the cross-view action recognition model, the learning approach should consider the following properties: (1) the geometric correlation between the third view and the first view has to be considered during the learning process, (2) the mechanism that guarantees the knowledge learned is well generalized from the third view to the first view.

#### 3.1. Cross-view Geometric Correlation in Attentions

With the success of Vision Transformer in action recognition [20, 49, 56], the self-attention mechanism is the key to learning the robust action recognition models. Therefore, in our work, we propose explicitly modeling cross-view learning in action recognition models through the self-attention mechanism. First, we revise the geometric correlation of the exocentric and egocentric views in obtaining the videos. Let us assume that  $\bar{\mathbf{x}}_{ego}$  is the corresponding egocentric video of the exocentric video  $\mathbf{x}_{exo}$ , and  $\mathbf{K}_{exo}, [\mathbf{R}_{exo}, \mathbf{t}_{exo}]$  and  $\mathbf{K}_{ego}, [\mathbf{R}_{ego}, \mathbf{t}_{ego}]$  are the camera (intrinsic and extrinsic) parameters of third and first views,

respectively. Then, the procedure of obtaining the videos can be formed as a rendering function as in Eqn. (2).

$$\begin{aligned}\mathbf{x}_{exo} &= \mathcal{R}(\mathbf{K}_{exo}, [\mathbf{R}_{exo}, \mathbf{t}_{exo}]) \\ \bar{\mathbf{x}}_{ego} &= \mathcal{R}(\mathbf{K}_{ego}, [\mathbf{R}_{ego}, \mathbf{t}_{ego}])\end{aligned}\quad (2)$$

where  $\mathcal{R}$  is a rendering function that obtains the video with the given corresponding camera matrix and position. In Eqn. (2), the rendering function  $\mathcal{R}$  remains the same across views as  $\mathbf{x}_{exo}$  and  $\bar{\mathbf{x}}_{ego}$  are the pair video of the same scene. Moreover, as the camera parameters are represented by matrices, there exist linear transformations of the cameras between two views defined as in Eqn. (3).

$$\begin{aligned}\mathbf{K}_{ego} &= \mathbf{T}_K \times \mathbf{K}_{exo} \\ [\mathbf{R}_{ego}, \mathbf{t}_{ego}] &= \mathbf{T}_{Rt} \times [\mathbf{R}_{exo}, \mathbf{t}_{exo}]\end{aligned}\quad (3)$$

**Remark 1: Cross-view Geometric Transformation** From Eqn. (2) and Eqn. (3), we have observed that there exists a geometric transformation  $\mathcal{T}$  of videos (images) between two camera views as follows:

$$\bar{\mathbf{x}}_{ego} = \mathcal{T}(\mathbf{x}_{exo}; \mathbf{T}_K, \mathbf{T}_{Rt}) \quad (4)$$

In our proposed method, we consider the action recognition backbone model  $F$  designed as a Transformer with self-attention layers. Given a video, the input of the Transformer is represented by  $N + 1$  tokens, including  $N = \frac{T}{K} \frac{H}{P} \frac{W}{P}$  non-overlapped patches ( $K \times P \times P$  is the patch size of the token) of a video and a single classification token. Let  $\mathbf{a}_{exo}, \bar{\mathbf{a}}_{ego} \in \mathbb{R}^{\frac{T}{K} \times \frac{H}{P} \times \frac{W}{P}}$  be an attention map of the video frames w.r.t the classification token extracted from the network  $F$  on the inputs  $\mathbf{x}_{exo}$  and  $\bar{\mathbf{x}}_{ego}$ , respectively. The attention maps  $\mathbf{a}_{exo}$  and  $\bar{\mathbf{a}}_{ego}$  represent the focus of the model on the video over time w.r.t to the model predictions. It should be noted the video and its attention map could be considered as a pixel-wised correspondence. Even though the patch size is greater than 1 ( $K, P > 1$ ), a single value in the attention map always corresponds to a group of pixels in its patch. Therefore, without a lack of generality, with the changes of cameras from the exocentric view to the eccentric view, we argue that the focuses of the model (the attention maps) also change correspondingly to the transitions of the videos across views because both videos are representing the same action scene from different camera views. As a result, the transformation between two attention maps, i.e.,  $\mathbf{a}_{exo}$  and  $\bar{\mathbf{a}}_{ego}$ , can also be represented by a transformation  $\mathcal{T}'$  w.r.t. the camera transformation matrices  $\mathbf{T}_K$  and  $\mathbf{T}_{Rt}$ .

**Remark 2: Cross-view Equivalent Transformation of Videos and Attentions** We argue that the transformations  $\mathcal{T}$  and  $\mathcal{T}'$  remain similar ( $\mathcal{T} \equiv \mathcal{T}'$ ) as they are both the transformation interpolation based on the camera transformation matrices  $\mathbf{T}_K$  and  $\mathbf{T}_{Rt}$ . Hence, the transformation  $\mathcal{T}$  could be theoretically adopted to the attention transformation.

$$\bar{\mathbf{a}}_{ego} = \mathcal{T}'(\mathbf{a}_{exo}; \mathbf{T}_K, \mathbf{T}_{Rt}) \equiv \mathcal{T}(\mathbf{a}_{exo}; \mathbf{T}_K, \mathbf{T}_{Rt}) \quad (5)$$

Followed by the above remarks, we further consider the cross-view correlation between the videos and the attention maps. Let  $\mathcal{D}_x(\mathbf{x}_{exo}, \bar{\mathbf{x}}_{ego})$  and  $\mathcal{D}_a(\mathbf{a}_{exo}, \bar{\mathbf{a}}_{ego})$  be the metrics measure the cross-view correlation in videos ( $\mathbf{x}_{exo}, \bar{\mathbf{x}}_{ego}$ ) and attention maps ( $\mathbf{a}_{exo}, \bar{\mathbf{a}}_{ego}$ ), respectively.

From Remark 1 and Remark 2, we have observed that the transformation of both video and attention from the exocentric view to the egocentric view is represented by the shared transformation  $\mathcal{T}$  and the camera transformation matrices  $\mathbf{T}_K, \mathbf{T}_{Rt}$ . In other words, the cross-view relation between  $\mathcal{D}_x(\mathbf{x}_{exo}, \bar{\mathbf{x}}_{ego})$  and  $\mathcal{D}_a(\mathbf{a}_{exo}, \bar{\mathbf{a}}_{ego})$  relies on the shared transformation  $\mathcal{T}(\cdot, \mathbf{T}_K, \mathbf{T}_{Rt})$  and the difference between  $\mathbf{x}_{exo}$  and  $\mathbf{a}_{exo}$ . Therefore, we argue that the cross-view video correlation  $\mathcal{D}_x(\mathbf{x}_{exo}, \bar{\mathbf{x}}_{ego})$  is theoretically proportional to the cross-view attention correlation  $\mathcal{D}_a(\mathbf{a}_{exo}, \bar{\mathbf{a}}_{ego})$ . In addition, the transformations between the two cameras are linear, as indicated in Eqn. (3). Thus, in our work, the proportion between  $\mathcal{D}_x(\mathbf{x}_{exo}, \bar{\mathbf{x}}_{ego})$  and  $\mathcal{D}_a(\mathbf{a}_{exo}, \bar{\mathbf{a}}_{ego})$  can be theorized as a linear relation and modeled by a linear scale  $\alpha$  as in Eqn. (6).

$$\begin{aligned}\mathcal{D}_x(\mathbf{x}_{exo}, \bar{\mathbf{x}}_{ego}) &\propto \mathcal{D}_a(\mathbf{a}_{exo}, \bar{\mathbf{a}}_{ego}) \\ \Leftrightarrow \mathcal{D}_x(\mathbf{x}_{exo}, \bar{\mathbf{x}}_{ego}) &= \alpha \mathcal{D}_a(\mathbf{a}_{exo}, \bar{\mathbf{a}}_{ego})\end{aligned}\quad (6)$$

### 3.2. Unpaired Cross-View Self-Attention Loss

Eqn. (6) defines a condition that explicitly models the self-attention correlation based on the geometric transformation across views. Thus, to efficiently learn the action recognition model from the exocentric to the egocentric view, Eqn (1) can be optimized w.r.t the condition in Eqn. (6) and presented as in Eqn. (7).

$$\begin{aligned}\arg \min_{\theta_F, \theta_{C_{exo}}, \theta_{C_{ego}}} & [\mathbb{E}_{\mathbf{x}_{exo}, \mathbf{y}_{ego}} \mathcal{L}_{ce}(C_{exo}(F(\mathbf{x}_{exo})), \mathbf{y}_{exo}) \\ & + \mathbb{E}_{\mathbf{x}_{ego}, \mathbf{y}_{ego}} \mathcal{L}_{ce}(C_{ego}(F(\mathbf{x}_{ego})), \mathbf{y}_{ego})] \\ \text{s.t.} \quad & \mathcal{D}_x(\mathbf{x}_{exo}, \bar{\mathbf{x}}_{ego}) = \alpha \mathcal{D}_a(\mathbf{a}_{exo}, \bar{\mathbf{a}}_{ego})\end{aligned}\quad (7)$$

Hence, optimizing Eqn. (7) can be solved by considering the cross-view constraint as a regularizer during training, i.e.,  $\|\mathcal{D}_x(\mathbf{x}_{exo}, \bar{\mathbf{x}}_{ego}) - \alpha \mathcal{D}_a(\mathbf{a}_{exo}, \bar{\mathbf{a}}_{ego})\|_2^2$ . However, it is noted that it requires a pair of third-view and first-view videos during training. Meanwhile, in practice, the video data of these two views are often recorded independently. Thus, optimizing Eqn. (7) by imposing the constraint of Eqn. (6) on pair data remains an ill-posed problem. Instead of solving Eqn. (7) on pair data, let us consider all cross-view unpaired samples ( $\mathbf{x}_{exo}, \mathbf{x}_{ego}$ ). In addition, we assume that the cross-view correlation of videos  $\mathcal{D}_x$  and attention maps  $\mathcal{D}_a$  is bounded by a certain threshold  $\beta$ , i.e.,  $\forall \mathbf{x}_{exp}, \mathbf{x}_{ego} : \mathcal{D}_x(\mathbf{x}_{exo}, \mathbf{x}_{ego}) \leq \beta$  and  $\forall \mathbf{a}_{exp}, \mathbf{a}_{ego} : \mathcal{D}_a(\mathbf{a}_{exo}, \mathbf{a}_{ego}) \leq \beta$ . This assumption implies that the distribution shifts (i.e., the changes of views) from the exocentric to the egocentric view are bounded to ensure that the model is able to generalize its capability



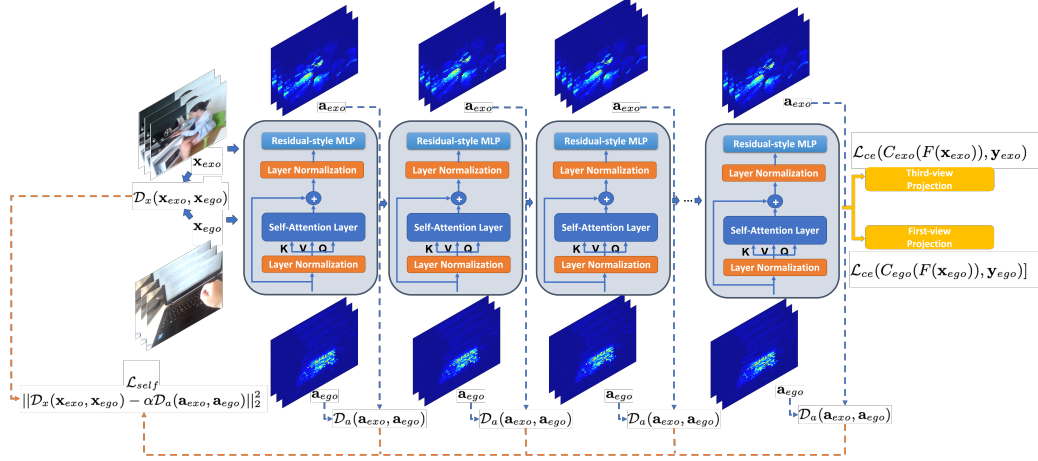


Figure 2. **The Proposed Framework.** The input videos  $\mathbf{x}_{exo}$  and  $\mathbf{x}_{ego}$  are first forwarded to Transformer  $F$  followed by the corresponding classifiers  $C_{exo}$  and  $C_{ego}$ , respectively. Then, the supervised cross-entropy loss  $\mathcal{L}_{ce}$  is applied to the predictions produced by the model. Meanwhile, the attention maps of video inputs, i.e.  $\mathbf{a}_{exo}$  and  $\mathbf{a}_{ego}$ , are extracted and imposed by the cross-view self-attention loss  $\mathcal{L}_{self}$ .

across views. Hence, our **Cross-view Self-Attention Loss** on unpaired data can be formulated as in Eqn. (8).

$$\mathcal{L}_{self} = \mathbb{E}_{\mathbf{x}_{exo}, \mathbf{x}_{ego}} \lambda \|\mathcal{D}_x(\mathbf{x}_{exo}, \mathbf{x}_{ego}) - \alpha \mathcal{D}_a(\mathbf{a}_{exo}, \mathbf{a}_{ego})\|_2^2 \quad (8)$$

where  $\lambda$  is the hyper-parameter controlling the relative importance of  $\mathcal{L}_{self}$ . Intuitively, even though the pair samples between exocentric and egocentric views are inaccessible, the cross-view constraints between videos and attention maps can still be imposed by modeling the topological constraint among unpaired samples. Furthermore, under our cross-view distribution shift assumption, our loss in Eqn. (8) can be proved as an upper bound of the constrain Eqn. (6) on pair samples as follows:

$$\begin{aligned} \mathcal{D}_x(\mathbf{x}_{exo}, \bar{\mathbf{x}}_{ego}) - \alpha \mathcal{D}_a(\mathbf{a}_{exo}, \bar{\mathbf{a}}_{ego}) \\ \leq \mathcal{D}_x(\mathbf{x}_{exo}, \mathbf{x}_{ego}) - \alpha \mathcal{D}_a(\mathbf{a}_{exo}, \mathbf{a}_{ego}) + (1 + \alpha)\beta \end{aligned} \quad (9)$$

Eqn. (13) can be proved using the triangle inequality property of  $\mathcal{D}_x$  and  $\mathcal{D}_a$ . It is detailed in the supplementary.

As shown in Eqn. (13), as  $\mathcal{D}_x(\mathbf{x}_{exo}, \mathbf{x}_{ego}) - \alpha \mathcal{D}_a(\mathbf{a}_{exo}, \mathbf{a}_{ego}) + (1 + \alpha)\beta$  is the upper bound of  $\mathcal{D}_x(\mathbf{x}_{exo}, \bar{\mathbf{x}}_{ego}) - \alpha \mathcal{D}_a(\mathbf{a}_{exo}, \bar{\mathbf{a}}_{ego})$ , minimizing  $\|\mathcal{D}_x(\mathbf{x}_{exo}, \mathbf{x}_{ego}) - \alpha \mathcal{D}_a(\mathbf{a}_{exo}, \mathbf{a}_{ego})\|_2^2$  also imposes the constraint of  $\|\mathcal{D}_x(\mathbf{x}_{exo}, \bar{\mathbf{x}}_{ego}) - \alpha \mathcal{D}_a(\mathbf{a}_{exo}, \bar{\mathbf{a}}_{ego})\|_2^2$ . Noted that  $\alpha$  and  $\beta$  are constant numbers, which can be excluded during training. Therefore, the constraints of cross-view correlation on pair samples in Eqn. (7) is guaranteed when optimizing  $\mathcal{L}_{self}$  defined in Eqn. (8). More importantly, our proposed cross-view self-attention loss **does NOT require the pair data between exocentric and egocentric views** during training. Fig. 2 illustrates our proposed cross-view learning framework.

**Cross-view Topological Preserving Property:** The proposed loss defined in Eqn. (8) to impose the cross-view correlation over all unpaired samples is a special case of the

Gromov-Wasserstein [61] distance between the video and the attention map distributions where the association matrix has been pre-defined. As a result, our loss inherits these Gromov-Wasserstein properties to preserve the topological distributions between the video and attention space. Particularly, the cross-view topological structures of video distributions are preserved in cross-view attention distributions.

### 3.3. The Choices of Correlation Metrics

As shown in Eqn. (8), the choice of correlation metric  $\mathcal{D}_x$  and  $\mathcal{D}_a$  is one of the primary factors directly influencing the performance of the action recognition models. The direct metrics, i.e.,  $\ell_2$ , could be straightforwardly adopted for the correlation metric  $\mathcal{D}_x$  and  $\mathcal{D}_a$ . However, this direct approach is ineffective because the deep semantic information of videos is not well modeled in the direct Euclidean metric  $\ell_s$ . To overcome this limitation, we first propose to design  $\mathcal{D}_x$  as the correlation metric on the deep latent spaces that can be defined as in Eqn. (10).

$$\mathcal{D}_x(\mathbf{x}_{exo}, \mathbf{x}_{ego}) = \mathcal{D}_x^G(\mathbf{x}_{exo}, \mathbf{x}_{ego}) = \|G(\mathbf{x}_{exo}) - G(\mathbf{x}_{ego})\|_2^2 \quad (10)$$

where  $G: \mathbb{R}^{T \times H \times W \times 3} \rightarrow \mathbb{R}^K$  be the deep network trained on the large-scale dataset. Intuitively, measuring the correlation between two videos provides a higher level of semantic information since the deep representation extracted by the large pre-trained model  $G$  capture more contextual information about the videos [40, 21].

As  $\mathcal{D}_a$  measures the correlation between two attention maps where each of that is in the form of the probability distribution,  $\mathcal{D}_a$  should be defined as the statistical distance to measure the correlation between two probabilistic attention maps comprehensively. Thus, we propose to design  $\mathcal{D}_a$

as the Jensen-Shannon divergence defined as in Eqn. (11).

$$\begin{aligned}\mathcal{D}_a(\mathbf{a}_{exo}, \mathbf{a}_{ego}) &= \mathcal{D}_a^{JS}(\mathbf{a}_{exo}, \mathbf{a}_{ego}) \\ &= \frac{1}{2}(\mathcal{D}_{KL}(\mathbf{a}_{exo}||\mathbf{a}_{ego}) + \mathcal{D}_{KL}(\mathbf{a}_{ego}||\mathbf{a}_{exo}))\end{aligned}\quad (11)$$

where  $\mathcal{D}_{KL}$  is the Kullback–Leibler divergence. To satisfy the cross-view distribution shift assumption aforementioned, the correlation metrics  $\mathcal{D}_x$  and  $\mathcal{D}_a$  are constrained by the threshold  $\beta$ , i.e.,  $\mathcal{D}_x(\mathbf{x}_{exo}, \mathbf{x}_{ego}) = \min(\mathcal{D}_x^G(\mathbf{x}_{exo}, \mathbf{x}_{ego}), \beta)$  and  $\mathcal{D}_a(\mathbf{a}_{exo}, \mathbf{a}_{ego}) = \min(\mathcal{D}_a^{JS}(\mathbf{a}_{exo}, \mathbf{a}_{ego}), \beta)$ . In our experiments, the value of  $\beta$  is set to 200.

## 4. Experimental Results

This section first briefly presents the datasets and the implementation details in our experiments. Then, we analyze the effectiveness of the approach in ablative experiments followed by comparing results with prior methods on the standard benchmarks of first-view action recognition.

### 4.1. Datasets and Implementation Details

Following the common practice in action recognition [26, 8, 56], Kinetics has been used as the third-view dataset in our experiment due to its large scale and diverse actions. To evaluate the effectiveness of our approach, we use EPIC-Kitchens and Charades-Ego as our first-view datasets. These two datasets are currently known as large-scale and challenging benchmarks in egocentric action recognition.

**Kinetics-400** [43] is a large-scale third-view action recognition dataset including 300K videos of 400 classes of human actions. The dataset is licensed by Google Inc. under a Creative Commons Attribution 4.0 International License.

**Charades-Ego** [72] is a first-view action recognition dataset that consists of 157 action classes with 68K clips. The license of Charades-Ego is registered for academic purposes by the Allen Institute for Artificial Intelligence.

**EPIC-Kitchens-55** [16] is a large-scale multi-task egocentric dataset of daily activities in kitchens. The action recognition task includes 55 hours of 39K clips and is annotated by interactions between 352 nouns and 125 verbs.

**EPIC-Kitchens-100** [15] is an larger version of the EPIC-Kitchens-55 where it is extended to 100 hours of 90k action clips. Each single action segment is annotated by an action of 97 verbs and 300 nouns. The EPIC Kitchens dataset was published under the Creative Commons Attribution-NonCommercial 4.0 International License.

**Evaluation Metrics** Our experiments follow the standard benchmarks of the Charades-Ego and EPIC-Kitchens for action recognition. We report the mean average precision (mAP) in the Charades-Ego [72] experiments and Top 1 and Top 5 accuracy of verb, noun, and action predictions of the validation set in EPIC-Kitchens [16, 15] experiments.

Table 1. Effectiveness of the Scale  $\alpha$  in the Linear Relation to the Charades-Ego (E-Ego) and EPIC-Kitchen-55 (EPIC) Action Recognition Benchmarks.

$\alpha$	C-Ego	EPIC Verb		EPIC Noun	
	mAP	Top 1	Top 5	Top 1	Top 5
0.00	20.70	41.94	67.31	43.19	60.14
0.25	25.09	55.96	89.37	55.96	80.65
0.50	28.97	58.84	87.24	54.75	75.27
0.75	<b>31.95</b>	60.80	89.62	57.42	77.77
1.00	30.68	68.97	89.53	44.87	70.98
1.50	29.51	<b>73.52</b>	<b>92.22</b>	<b>68.19</b>	<b>84.93</b>
2.00	27.80	69.60	92.54	61.60	81.22

**Implementation** In our work, we adopt the design of the Vision Transformation Base model (ViT-B) [20] for our Transformer backbone. Our model is implemented in Python using the PyTorch and PySlowFast [23] frameworks. The input video of our network consists of  $T = 16$  frames sampled at the frame rate of  $1/4$  and the input resolution of each video frame is  $H \times W = 224 \times 224$ . Each video is tokenized by the non-overlapping patch size of  $K \times P \times P = 2 \times 16 \times 16$ . Each token is projected by an embedding where the dimension length of the embedding is set to 768. There are 12 Transformer layers in our model and the number of heads in each self-attention layer is set to 8. The entire framework is optimized by the Stochastic Gradient Descent algorithm, where our models are trained for 50 epochs. The cosine learning policy is utilized in our training, where the base learning rate is set to 0.00125. Similar to [49, 26], to increase the diversity of training data, we also apply several augmentation methods during training. All of our models are trained on the four 40GB-VRAM A100 GPUs, and the batch size in each GPU is set to 4. Swin-B [56] pre-trained on the Kinetics-400 dataset has been adopted for our network  $G$  in Eqn. (10). Since we do not want the gradients produced by the supervised loss  $\mathcal{L}_{ce}$  being suppressed by the cross-view loss  $\mathcal{L}_{self}$ , the hyper-parameter  $\lambda$  is set to  $5.10^{-3}$ . In our evaluation, following prior works [8, 48], each input is sampled in the middle of the video. The final result is obtained by averaging the prediction scores of three spatial crops, i.e., top-left, center, and bottom-right, from the video input.

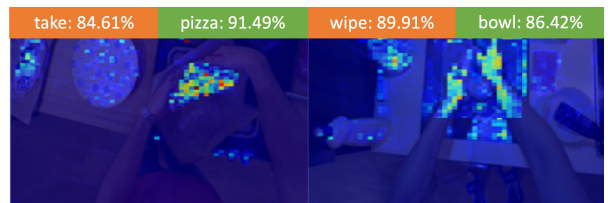


Figure 3. Attention Visualization of Model Prediction (verb and noun) on EPIC Kitchen Videos.

Table 2. Effectiveness of the Choices of Correlation Metrics to the Charades-Ego (E-Ego) and EPIC-Kitchen-55 (EPIC) Action Recognition Benchmarks.

$\mathcal{D}_x$		$\mathcal{D}_a$		C-Ego	EPIC Verb		EPIC Noun	
$\ell_2$	$\mathcal{D}_x^G$	$\ell_2$	$\mathcal{D}_a^{JS}$	mAP	Top 1	Top 5	Top 1	Top 5
✓		✓		27.80	60.97	89.95	58.05	78.07
✓			✓	28.77	61.13	90.16	58.05	78.40
	✓	✓		29.11	63.13	90.12	59.68	80.03
	✓		✓	<b>31.95</b>	<b>73.52</b>	<b>92.22</b>	<b>68.19</b>	<b>84.93</b>

## 4.2. Ablation Studies

Our ablative experiments report the results of our CVAR method with different settings trained on the Kinetics-400  $\rightarrow$  Charades-Ego and Kinetics-400  $\rightarrow$  EPIC-Kitchens-55 benchmarks. For fair comparisons, all the models are trained with the same learning configuration.

**Effectiveness of the scale  $\alpha$**  We study the effectiveness of the linear scale  $\alpha$  to the performance of the model. In this experiment, the metrics defined in Eqn. (10) and Eqn. (11) have been adopted to  $\mathcal{D}_x$  and  $\mathcal{D}_a$ . The value  $\alpha$  ranges from 0.0 to 2.0. When  $\alpha = 0.0$ , it is equivalent to ViT simultaneously trained on both third-view and first-view datasets. As shown in Table 1, the mAP performance on the Charades-Ego benchmark is consistently improved when the value of  $\alpha$  increases from 0.1 to 0.75 and achieves the best performance at the value of  $\alpha = 0.75$  and the mAP performance is 31.95%. Similarly, on the EPIC-Kitchen-55 benchmarks, the Top 1 and Top 5 accuracy is gradually improved w.r.t the increasing of  $\alpha$  and reaches the maximum performance when the value of  $\alpha$  is 1.50 in which the Top 1 accuracy on EPIC Verb and EPIC Noun are 73.52% and 68.19%. Then, the performance on both benchmarks inclines to steadily decrease when the value of  $\alpha$  keeps increasing over the optimal point. Indeed, the variation in the video space is typically higher than in the attention maps due to the higher complexity of video data where the video data contains much more information, e.g., objects, humans, and interactions, etc.; meanwhile, the attention maps represent the focus of the models w.r.t model decisions. Thus, if the value of  $\alpha$  is small, it could not represent the correct proportion of changes between videos and attention maps. Meanwhile, the higher value of  $\alpha$  inclines to exaggerate the model focuses, i.e., attention maps, that results in the performance.

Table 3. Effectiveness of the Transformer Layers to the Charades-Ego (E-Ego) and EPIC-Kitchen-55 (EPIC) Action Recognition Benchmarks.

Transformer Layers				C-Ego	EPIC Verb		EPIC Noun	
1-3	4-6	7-9	10-12	mAP	Top 1	Top 5	Top 1	Top 5
✓				25.65	60.47	90.26	57.85	78.58
✓	✓			28.19	68.46	91.08	66.54	83.36
✓	✓	✓		30.60	69.27	<b>92.58</b>	68.09	<b>85.02</b>
✓	✓	✓	✓	<b>31.95</b>	<b>73.52</b>	92.22	<b>68.19</b>	84.93

Table 4. Comparisons on Charades-Ego.

Method	mAP
ActorObserverNet [71]	20.00
SSDA [13]	23.10
I3D [13]	25.80
DANN [33]	23.62
SlowFast [26]	25.93
Frozen [6]	28.80
MViT-V2	25.65
Swin-B [56]	28.77
Ego-Exo + ResNet-50 [48]	26.23
Ego-Exo + SlowFast R50 [48]	28.04
Ego-Exo* + ResNet-50 [48]	27.47
Ego-Exo* + SlowFast R50 [48]	29.19
Ego-Exo* + SlowFast R101 [48]	30.13
<b>CVAR (Ours)</b>	<b>31.95</b>

**Effectiveness of the metrics** This experiment studies the effectiveness of correlation metrics to the performance of the action recognition models on first-view videos. The optimal value of the linear  $\alpha$  in the previous ablation study has been adopted in this experiment. For each metric correlation, we study its effect by comparing the performance of action recognition models using our metric in Eqn. (10) and Eqn. (11) against the Euclidean distance  $\ell_2$ . As our results in Table 2, by measuring the correlation of videos on the deep latent spaces, i.e.,  $\mathcal{D}_x^G$ , the performance of the action recognition model has been improved, e.g., 28.77% to 31.95% (results using  $\mathcal{D}_a^{JS}$ ). This improvement is gained thanks to the deep semantic representation extracted by deep network  $G$ . Besides, the probability metric used to measure the correlation between attention maps, i.e.,  $\mathcal{D}_a^{JS}$ , has illustrated its significant role. For example, the performance of the model has been promoted by +2.84% from 29.11% (using  $\ell_2$ ) to 31.95% (using  $\mathcal{D}_a^{JS}$ ). As the attention map is in the form of the probability distribution, using the Jensen-Shannon divergence as the correlation metric provides the informative difference of the model’s focus over the videos. Meanwhile,  $\ell_2$  tends to rely on the difference of the magnitude of the attention, which provides less correlation information between two attentions.

**Effectiveness of Transformer Layers** This experiment

Table 5. Comparisons on EPIC-Kitchen-55.

Method	EPIC verbs		EPIC nouns	
	Top 1	Top 5	Top 1	Top 5
ResNet-50 [26]	61.19	87.49	46.18	69.72
MViT-V2 [49]	55.17	89.87	56.59	79.40
Swin-B [56]	56.40	85.84	47.68	71.02
DANN [33]	61.27	87.49	45.93	68.73
Joint-Embed [71]	61.26	87.17	46.55	68.97
Ego-Exo + ResNet-50 [48]	62.83	87.63	48.15	70.28
Ego-Exo + SlowFast [48]	65.97	88.91	49.42	72.35
Ego-Exo* + ResNet-50 [48]	64.26	88.45	48.39	70.68
Ego-Exo* + SlowFast [48]	66.43	89.16	49.79	71.60
<b>CVAR (Ours)</b>	<b>73.52</b>	<b>92.22</b>	<b>68.19</b>	<b>84.93</b>

Table 6. Comparisons to Prior Methods on the EPIC-Kitchen-100 Action Recognition Benchmark.

Method	Overall						Unseen Participants			Tail Classes		
	Top-1 Accuracy			Top-5 Accuracy			Top-1 Accuracy			Top-1 Accuracy		
	Verb	Noun	Action	Verb	Noun	Action	Verb	Noun	Action	Verb	Noun	Action
TSN [86]	60.18	46.03	33.19	89.59	72.90	55.13	47.42	38.03	23.47	30.45	19.37	13.88
TRN [93]	65.88	45.43	35.34	90.42	71.88	56.74	55.96	37.75	27.70	34.66	17.58	14.07
TBN [45]	66.00	47.23	36.72	90.46	73.76	57.66	59.44	38.22	29.48	39.09	24.84	19.13
TSM [50]	67.86	49.01	38.27	90.98	74.97	60.41	58.69	39.62	29.48	36.59	23.37	17.62
SlowFast [26]	65.56	50.02	38.54	90.00	75.62	58.60	56.43	41.50	29.67	36.19	23.26	18.81
MViT-V2 [49]	67.13	60.89	45.79	91.13	83.93	66.83	57.75	50.52	34.84	40.85	38.47	25.35
Ego-Exo [48]	66.61	59.51	44.89	91.13	82.03	65.05	56.57	48.87	33.71	40.91	38.26	25.23
Swin-B [56]	67.93	58.69	46.05	90.96	<b>83.77</b>	65.23	58.69	<b>50.89</b>	35.02	41.08	37.21	25.41
<b>CVAR (Ours)</b>	<b>69.37</b>	<b>61.03</b>	<b>46.15</b>	<b>91.51</b>	81.03	<b>67.05</b>	<b>59.91</b>	48.36	<b>35.12</b>	<b>41.93</b>	<b>38.58</b>	<b>25.99</b>

studies the effectiveness of imposing the cross-view loss into attention maps of the Transformer layers. In this experiment, we adopt the optimal setting of the linear scale ( $\alpha$ ) and correlation metrics ( $\mathcal{D}_x$ ,  $\mathcal{D}_a$ ) in the previous ablation studies. We consider four groups of Transformer layers where each group consists of three consecutive layers, i.e., Layer 1-3, Layer 4-6, Layer 7-9, and Layer 10-12. As experimental results in Table 3, the later Transformer layers of our model play an important role than the initial ones. In particular, when imposing the cross-view loss on only the first three Transformer layers, the performance of Charades-Ego has achieved 25.65% and the Top 1 accuracy of verb and noun predictions in EPIC-Kitchens-55 is 60.47% and 57.85%. Meanwhile, enforcing the cross-view self-attention loss into all attention layers brings better performance and achieves the best performance, i.e., the mAP of 31.95% on Charades-Ego and Top 1 accuracy of 73.52% and 68.19% on EPIC-Kitchens-55. Fig. 3 visualizes the attention maps of the model predictions.

### 4.3. Comparisons with State-of-the-Art Results

**Kinetics-400  $\rightarrow$  Charades-Ego** Table 4 presents results of our CVAR compared to prior methods, i.e., ActorObserverNet [71], SSDA [13], I3D [13], DANN [33], SlowFast [26], Frozen [6], MViT-V2 [49], Swin-B [56], and Ego-Exo [48], on the Charades-Ego benchmark. Our results in Table 4 have gained SOTA performance where our mAP accuracy in our approach has achieved 31.95%. Compared to direct training approaches [20, 6, 56, 24, 13], our method achieves better performance than other methods by a large margin, e.g., higher than Swin-B [56] by 3.18%. In comparison with the prior pre-training approach using additional egocentric tasks, our result is higher than Ego-Exo [48] by +1.82%. Meanwhile, compared with domain adaptation approaches [33, 13], our methods outperform DANN by +8.33%.

**Kinetics-400  $\rightarrow$  EPIC-Kitchens-55** Table 5 presents the results of our approach compared to prior methods, i.e., ResNet-50 [26], DANN [33], SlowFast [26], MViT-V2 [49], Swin-B [56], and Ego-Exo [48], on the EPIC-Kitchens-55 benchmark. Our proposed CVAR has gained

the SOTA performance where our Top 1 accuracy on EPIC Verb and EPIC Noun of our approach has achieved 73.52% and 68.19%, respectively. Our proposed approach outperforms the traditional direct training approaches [26, 49, 56] by a large margin. In addition, our result is higher than the pre-training approach using additional egocentric tasks, i.e., Ego-Exo [48], by +6.48% and +18.4% on Top 1 accuracy of verb and noun predictions. Our method also outperforms the domain adaptation approach [33].

**Kinetics-400  $\rightarrow$  EPIC-Kitchens-100** Table 6 compares our results with TSN [86], TRN [93], TBN [45], TSM [50], SlowFast [26], MViT-V2 [49], Ego-Exo using SlowFast-R50 [48], and Swin-B [56] on the EPIC-Kitchens-100 benchmark. Overall, our proposed CVAR has achieved the SOTA performance where the Top 1 accuracy of verb, noun, and action predictions are 69.37%, 61.03%, and 46.15%, respectively. Also, CVAR has gained competitive performance on the sets of unseen participants and tail classes. Compared to prior direct training methods [56, 49, 20], our method outperforms these approaches by a notable margin, i.e. higher than Swin-B by +1.44% and +2.34% on Top 1 Accuracy of Verb and Noun predictions in overall. Also, our results outperform Ego-Exo in not only overall accuracy but also in unseen participants and tail classes.

## 5. Conclusions and Limitations

**Conclusions** This paper presents a novel approach for cross-view learning in action recognition (CVAR). By using our proposed cross-view self-attention loss, our approach has effectively transferred the knowledge learned from the exocentric to the egocentric view. Moreover, our approach does not require pairs of videos across views which increases the flexibility of our learning approaches in practice. Experimental results on standard egocentric action recognition benchmarks, have shown our SOTA performance. Particularly, our method outperforms the prior direct training, pre-training, and domain adaptation methods.

**Limitation of Linear Relation** Modeling the relation in Eqn. (6) by the linear scale  $\alpha$  could bring some potential limitations as the cross-view correlation of videos and at-



tention maps could be a non-linear proportion and may be subjected to an individual video and its corresponding attention map. Our future works will consider modeling this relation by a deep network to gain more improvement.

**Limitation of Bounded Distribution Shifts** Although this assumption allows us to establish the bounded constraint as in Eqn. (13) and further derive into our loss in Eqn. (8), this could also contain some potential limitations. If the changes across views of videos (attention maps) are significantly large, this could result in the bounded constraint in Eqn. (13) is not tight. Thus, the models could not be well generalized w.r.t the large distribution shifts.

## References

- [1] Shervin Ardeshtir and Ali Borji. Ego2top: Matching viewers in egocentric and top-view videos. In *ECCV*, 2016. 3
- [2] Shervin Ardeshtir and Ali Borji. An exocentric look at egocentric actions and vice versa. *Computer Vision and Image Understanding*, 171, 2018. 3
- [3] Shervin Ardeshtir and Ali Borji. Integrating egocentric videos in top-view surveillance videos: Joint identification and temporal alignment. In *ECCV*, 2018. 3
- [4] Shervin Ardeshtir, Sandesh Sharma, and Ali Broji. Egoreid: Cross-view self-identification and human re-identification in egocentric and surveillance videos. *arXiv preprint arXiv:1612.08153*, 2016. 3
- [5] Anurag Arnab, Mostafa Dehghani, Georg Heigold, Chen Sun, Mario Lučić, and Cordelia Schmid. Vivit: A video vision transformer, 2021. 2
- [6] Max Bain, Arsha Nagrani, Gül Varol, and Andrew Zisserman. Frozen in time: A joint video and image encoder for end-to-end retrieval. In *IEEE International Conference on Computer Vision*, 2021. 7, 8
- [7] Fabien Baradel, Natalia Neverova, Christian Wolf, Julien Mille, and Greg Mori. Object level visual reasoning in videos. In *ECCV*, 2018. 3
- [8] Gedas Bertasius, Heng Wang, and Lorenzo Torresani. Is space-time attention all you need for video understanding? In *Proceedings of the International Conference on Machine Learning (ICML)*, July 2021. 2, 6
- [9] Adrian Bulat, Juan-Manuel Perez-Rua, Swathikiran Sudhakaran, Brais Martinez, and Georgios Tzimiropoulos. Space-time mixing attention for video transformer. In A. Beygelzimer, Y. Dauphin, P. Liang, and J. Wortman Vaughan, editors, *Advances in Neural Information Processing Systems*, 2021. 2
- [10] João Carreira, Eric Noland, Andras Banki-Horvath, Chloe Hillier, and Andrew Zisserman. A short note about kinetics-600. *CoRR*, abs/1808.01340, 2018. 2
- [11] João Carreira, Eric Noland, Chloe Hillier, and Andrew Zisserman. A short note on the kinetics-700 human action dataset. *CoRR*, abs/1907.06987, 2019. 1, 2
- [12] João Carreira and Andrew Zisserman. Quo vadis, action recognition? A new model and the kinetics dataset. In *CVPR*, pages 4724–4733. IEEE, 2017. 2
- [13] Jinwoo Choi, Gaurav Sharma, Manmohan Chandraker, and Jia-Bin Huang. Unsupervised and semi-supervised domain adaptation for action recognition from drones. In *WACV*, 2020. 3, 7, 8
- [14] Benjamin Coors, Alexandru Paul Condurache, and Andreas Geiger. Nova: Learning to see in novel viewpoints and domains. In *2019 International Conference on 3D Vision (3DV)*, pages 116–125, 2019. 3
- [15] Dima Damen, Hazel Doughty, Giovanni Maria Farinella, Antonino Furnari, Jian Ma, Evangelos Kazakos, Davide Moltisanti, Jonathan Munro, Toby Perrett, Will Price, and Michael Wray. Rescaling egocentric vision. *CoRR*, abs/2006.13256, 2020. 1, 2, 3, 6
- [16] Dima Damen, Hazel Doughty, Giovanni Maria Farinella, Sanja Fidler, Antonino Furnari, Evangelos Kazakos, Davide Moltisanti, Jonathan Munro, Toby Perrett, Will Price, et al. Scaling egocentric vision: The epic-kitchens dataset. In *ECCV*, 2018. 2, 3, 6
- [17] Eadom Dessalene, Michael Maynord, Chinmaya Devaraj, Cornelia Fermüller, and Yiannis Aloimonos. Egocentric object manipulation graphs. *arXiv preprint arXiv:2006.03201*, 2020. 3
- [18] Daniele Di Mauro, Antonino Furnari, Giuseppe Patanè, Sebastiano Battiato, and Giovanni Maria Farinella. Sceneadapt: Scene-based domain adaptation for semantic segmentation using adversarial learning. *Pattern Recognition Letters*, 136:175–182, 2020. 3
- [19] Jeff Donahue, Lisa Anne Hendricks, Sergio Guadarrama, Marcus Rohrbach, Subhashini Venugopalan, Trevor Darrell, and Kate Saenko. Long-term recurrent convolutional networks for visual recognition and description. In *CVPR*, pages 2625–2634. IEEE, 2015. 2
- [20] Alexey Dosovitskiy, Lucas Beyer, Alexander Kolesnikov, Dirk Weissenborn, Xiaohua Zhai, Thomas Unterthiner, Mostafa Dehghani, Matthias Minderer, Georg Heigold, Sylvain Gelly, Jakob Uszkoreit, and Neil Houlsby. An image is worth 16x16 words: Transformers for image recognition at scale, 2021. 2, 3, 6, 8
- [21] Chi Nhan Duong, Thanh-Dat Truong, Khoa Luu, Kha Gia Quach, Hung Bui, and Kaushik Roy. Vec2face: Unveil human faces from their blackbox features in face recognition. In *CVPR*, 2020. 5
- [22] Mohamed Elfeki, Krishna Regmi, Shervin Ardeshtir, and Ali Borji. From third person to first person: Dataset and baselines for synthesis and retrieval. *arXiv preprint arXiv:1812.00104*, 2018. 3
- [23] Haoqi Fan, Yanghao Li, Bo Xiong, Wan-Yen Lo, and Christoph Feichtenhofer. Pyslowfast. <https://github.com/facebookresearch/slowfast>, 2020. 6
- [24] Haoqi Fan, Bo Xiong, Kartikeya Mangalam, Yanghao Li, Zhicheng Yan, Jitendra Malik, and Christoph Feichtenhofer. Multiscale vision transformers, 2021. 2, 8
- [25] Christoph Feichtenhofer. X3d: Expanding architectures for efficient video recognition, 2020. 2
- [26] Christoph Feichtenhofer, Haoqi Fan, Jitendra Malik, and Kaiming He. Slowfast networks for video recognition. In *ICCV*, pages 6201–6210. IEEE, 2019. 1, 2, 3, 6, 7, 8

- [27] Christoph Feichtenhofer, Axel Pinz, and Richard P. Wildes. Spatiotemporal residual networks for video action recognition. In Daniel D. Lee, Masashi Sugiyama, Ulrike von Luxburg, Isabelle Guyon, and Roman Garnett, editors, *NeurIPS*, pages 3468–3476, 2016. 2
- [28] Christoph Feichtenhofer, Axel Pinz, and Richard P. Wildes. Spatiotemporal multiplier networks for video action recognition. In *CVPR*, pages 7445–7454. IEEE, 2017. 2
- [29] Christoph Feichtenhofer, Axel Pinz, and Andrew Zisserman. Convolutional two-stream network fusion for video action recognition. In *CVPR*, pages 1933–1941. IEEE, 2016. 2
- [30] A. Furnari, S. Battiato, K. Grauman, and G. Maria Farinella. Next-active-object prediction from egocentric videos. *Journal of Visual Communication and Image Representation*, 2017. 1, 3
- [31] Antonino Furnari and Giovanni Farinella. Rolling-unrolling lstms for action anticipation from first-person video. *IEEE Transactions on Pattern Analysis and Machine Intelligence*, 2020. 3
- [32] Antonino Furnari and Giovanni Maria Farinella. What would you expect? anticipating egocentric actions with rolling-unrolling lstms and modality attention. In *ICCV*, 2019. 3
- [33] Yaroslav Ganin, Evgeniya Ustinova, Hana Ajakan, Pascal Germain, Hugo Larochelle, François Laviolette, Mario Marchand, and Victor Lempitsky. Domain-adversarial training of neural networks. *The Journal of Machine Learning Research*, 17(1), 2016. 2, 3, 7, 8
- [34] Raghav Goyal, Samira Ebrahimi Kahou, Vincent Michalski, Joanna Materzyńska, Susanne Westphal, Heuna Kim, Valentin Haenel, Ingo Fruend, Peter Yianilos, Moritz Mueller-Freitag, Florian Hoppe, Christian Thureau, Ingo Bax, and Roland Memisevic. The “something something” video database for learning and evaluating visual common sense, 2017. 2
- [35] Kristen Grauman, Andrew Westbury, Eugene Byrne, Zachary Chavis, Antonino Furnari, Rohit Girdhar, Jackson Hamburger, Hao Jiang, Miao Liu, Xingyu Liu, Miguel Martin, Tushar Nagarajan, Ilija Radosavovic, Santhosh Kumar Ramakrishnan, Fiona Ryan, Jayant Sharma, Michael Wray, Mengmeng Xu, Eric Zhongcong Xu, Chen Zhao, Siddhant Bansal, Dhruv Batra, Vincent Cartillier, Sean Crane, Tien Do, Morrie Doulaty, Akshay Erapalli, Christoph Feichtenhofer, Adriano Fragomeni, Qichen Fu, Christian Fuegen, Abraham Gebreselasie, Cristina Gonzalez, James Hillis, Xuhua Huang, Yifei Huang, Wenqi Jia, Weslie Khoo, Jachym Kolar, Satwik Kottur, Anurag Kumar, Federico Landini, Chao Li, Yanghao Li, Zhenqiang Li, Karttikeya Mangalam, Raghava Modhugu, Jonathan Munro, Tullie Murrell, Takumi Nishiyasu, Will Price, Paola Ruiz Puentes, Merey Ramazanov, Leda Sari, Kiran Somasundaram, Audrey Southerland, Yusuke Sugano, Ruijie Tao, Minh Vo, Yuchen Wang, Xindi Wu, Takuma Yagi, Yunyi Zhu, Pablo Arbelaez, David Crandall, Dima Damen, Giovanni Maria Farinella, Bernard Ghanem, Vamsi Krishna Ithapu, C. V. Jawahar, Hanbyul Joo, Kris Kitani, Haizhou Li, Richard Newcombe, Aude Oliva, Hyun Soo Park, James M. Rehg, Yoichi Sato, Jianbo Shi, Mike Zheng Shou, Antonio Torralba, Lorenzo Torresani, Mingfei Yan, and Jitendra Malik. Ego4d: Around the World in 3,000 Hours of Egocentric Video. In *IEEE/CVF Computer Vision and Pattern Recognition (CVPR)*, 2022. 2, 3
- [36] Chunhui Gu, Chen Sun, David A. Ross, Carl Vondrick, Caroline Pantofaru, Yeqing Li, Sudheendra Vijayanarasimhan, George Toderici, Susanna Ricco, Rahul Sukthankar, Cordelia Schmid, and Jitendra Malik. AVA: A video dataset of spatio-temporally localized atomic visual actions. In *CVPR*, pages 6047–6056. IEEE, 2018. 2
- [37] Kaiming He, Xiangyu Zhang, Shaoqing Ren, and Jian Sun. Deep residual learning for image recognition. In *CVPR*, pages 770–778. IEEE, 2016. 2
- [38] Roei Herzig, Elad Ben-Avraham, Karttikeya Mangalam, Amir Bar, Gal Chechik, Anna Rohrbach, Trevor Darrell, and Amir Globerson. Object-region video transformers. In *Proceedings of the IEEE/CVF Conference on Computer Vision and Pattern Recognition (CVPR)*, pages 3148–3159, June 2022. 1
- [39] Sepp Hochreiter and Jürgen Schmidhuber. Long short-term memory. *Neural Comput.*, 9(8):1735–1780, 1997. 2
- [40] Justin Johnson, Alexandre Alahi, and Li Fei-Fei. Perceptual losses for real-time style transfer and super-resolution. In *European conference on computer vision*, pages 694–711. Springer, 2016. 5
- [41] Georgios Kipidis, Ronald Poppe, Elsbeth Van Dam, Lucas Noldus, and Remco Veltkamp. Egocentric hand track and object-based human action recognition. In *IEEE SmartWorld, Ubiquitous Intelligence & Computing, Advanced & Trusted Computing, Scalable Computing & Communications, Cloud & Big Data Computing, Internet of People and Smart City Innovation (SmartWorld/SCALCOM/UIC/ATC/CBDCOM/IOP/SCI)*, 2019. 3
- [42] Andrej Karpathy, George Toderici, Sanketh Shetty, Thomas Leung, Rahul Sukthankar, and Fei-Fei Li. Large-scale video classification with convolutional neural networks. In *CVPR*, pages 1725–1732. IEEE, 2014. 2
- [43] Will Kay, Joao Carreira, Karen Simonyan, Brian Zhang, Chloe Hillier, Sudheendra Vijayanarasimhan, Fabio Viola, Tim Green, Trevor Back, Paul Natsev, et al. The kinetics human action video dataset. *arXiv preprint arXiv:1705.06950*, 2017. 6
- [44] Will Kay, João Carreira, Karen Simonyan, Brian Zhang, Chloe Hillier, Sudheendra Vijayanarasimhan, Fabio Viola, Tim Green, Trevor Back, Paul Natsev, Mustafa Suleyman, and Andrew Zisserman. The kinetics human action video dataset. *CoRR*, abs/1705.06950, 2017. 2
- [45] Evangelos Kazakos, Arsha Nagrani, Andrew Zisserman, and Dima Damen. Epic-fusion: Audio-visual temporal binding for egocentric action recognition. In *ICCV*, 2019. 3, 8
- [46] Haoxin Li, Wei-Shi Zheng, Jianguo Zhang, Haifeng Hu, Jiwen Lu, and Jian-Huang Lai. Egocentric action recognition by automatic relation modeling. *IEEE Transactions on Pattern Analysis and Machine Intelligence*, 45(1):489–507, 2023. 1
- [47] Yin Li, Miao Liu, and James M Rehg. In the eye of beholder: Joint learning of gaze and actions in first person video. In *ECCV*, 2018. 3

- [48] Yanghao Li, Tushar Nagarajan, Bo Xiong, and Kristen Grauman. Ego-exo: Transferring visual representations from third-person to first-person videos. In *CVPR*, 2021. 1, 2, 3, 6, 7, 8
- [49] Yanghao Li, Chao-Yuan Wu, Haoqi Fan, Karttikeya Mangalam, Bo Xiong, Jitendra Malik, and Christoph Feichtenhofer. Mvitv2: Improved multiscale vision transformers for classification and detection. In *CVPR*, 2022. 1, 2, 3, 6, 7, 8
- [50] Ji Lin, Chuang Gan, and Song Han. Tsm: Temporal shift module for efficient video understanding. In *ICCV*, 2019. 2, 8
- [51] Kevin Qinghong Lin, Alex Jinpeng Wang, Mattia Soldan, Michael Wray, Rui Yan, Eric Zhongcong Xu, Difei Gao, Rongcheng Tu, Wenzhe Zhao, Weijie Kong, et al. Egocentric video-language pretraining. *arXiv preprint arXiv:2206.01670*, 2022. 1, 2, 3
- [52] Gaowen Liu, Hao Tang, Hugo Latapie, and Yan Yan. Exocentric to egocentric image generation via parallel generative adversarial network. In *ICASSP*, 2020. 3
- [53] Miao Liu, Siyu Tang, Yin Li, and James Rehg. Forecasting human object interaction: Joint prediction of motor attention and egocentric activity. *arXiv preprint arXiv:1911.10967*, 2019. 3
- [54] Tianshan Liu and Kin-Man Lam. A hybrid egocentric activity anticipation framework via memory-augmented recurrent and one-shot representation forecasting. In *Proceedings of the IEEE/CVF Conference on Computer Vision and Pattern Recognition (CVPR)*, pages 13904–13913, June 2022. 1
- [55] Yunze Liu, Yun Liu, Che Jiang, Kangbo Lyu, Weikang Wan, Hao Shen, Boqiang Liang, Zhoujie Fu, He Wang, and Li Yi. Hoi4d: A 4d egocentric dataset for category-level human-object interaction. In *Proceedings of the IEEE/CVF Conference on Computer Vision and Pattern Recognition (CVPR)*, pages 21013–21022, June 2022. 2
- [56] Ze Liu, Jia Ning, Yue Cao, Yixuan Wei, Zheng Zhang, Stephen Lin, and Han Hu. Video swin transformer, 2021. 1, 2, 3, 6, 7, 8
- [57] Minlong Lu, Danping Liao, and Ze-Nian Li. Learning spatiotemporal attention for egocentric action recognition. In *ICCV Workshops*, 2019. 3
- [58] Minghuang Ma, Haoqi Fan, and Kris M Kitani. Going deeper into first-person activity recognition. In *CVPR*, 2016. 3
- [59] Stefan Mathe and Cristian Sminchisescu. Dynamic eye movement datasets and learnt saliency models for visual action recognition. In *ECCV*, 2012. 3
- [60] Tushar Nagarajan, Yanghao Li, Christoph Feichtenhofer, and Kristen Grauman. Ego-topo: Environment affordances from egocentric video. In *CVPR*, 2020. 3
- [61] Gabriel Peyré and Marco Cuturi. Computational optimal transport. 2018. 5
- [62] Fiora Pirri, Lorenzo Mauro, Edoardo Alati, Valsamis Ntouskos, Mahdiah Izadpanahkakhk, and Elham Omrani. Anticipation and next action forecasting in video: an end-to-end model with memory. *arXiv preprint arXiv:1901.03728*, 2019. 3
- [63] Zhaofan Qiu, Ting Yao, and Tao Mei. Learning spatiotemporal representation with pseudo-3d residual networks. In *ICCV*, pages 5534–5542. IEEE, 2017. 2
- [64] Krishna Regmi and Ali Borji. Cross-view image synthesis using conditional gans. In *CVPR*, 2018. 3
- [65] Krishna Regmi and Mubarak Shah. Bridging the domain gap for ground-to-aerial image matching. In *ICCV*, 2019. 3
- [66] Hanxiang Ren, Yanchao Yang, He Wang, Bokui Shen, Qingnan Fan, Youyi Zheng, C. Karen Liu, and Leonidas Guibas. Adela: Automatic dense labeling with attention for view-point shift in semantic segmentation. In *2022 IEEE/CVF Conference on Computer Vision and Pattern Recognition (CVPR)*, pages 8069–8079, 2022. 3
- [67] Dandan Shan, Jiaqi Geng, Michelle Shu, and David F Fouhey. Understanding human hands in contact at internet scale. In *CVPR*, 2020. 3
- [68] Jinghuan Shang, Srijan Das, and Michael S Ryoo. Learning viewpoint-agnostic visual representations by recovering tokens in 3d space. In Alice H. Oh, Alekh Agarwal, Danielle Belgrave, and Kyunghyun Cho, editors, *Advances in Neural Information Processing Systems*, 2022. 3
- [69] Yujiao Shi, Liu Liu, Xin Yu, and Hongdong Li. Spatial-aware feature aggregation for image based cross-view geolocalization. In H. Wallach, H. Larochelle, A. Beygelzimer, F. d’Alch’e-Buc, E. Fox, and R. Garnett, editors, *Advances in Neural Information Processing Systems 32*, pages 10090–10100. Curran Associates, Inc., 2019. 3
- [70] Yujiao Shi, Xin Yu, Dylan Campbell, and Hongdong Li. Where am i looking at? joint location and orientation estimation by cross-view matching. In *Proceedings of the IEEE Conference on Computer Vision and Pattern Recognition*, 2020. 3
- [71] Gunnar A Sigurdsson, Abhinav Gupta, Cordelia Schmid, Ali Farhadi, and Karteek Alahari. Actor and observer: Joint modeling of first and third-person videos. In *CVPR*, 2018. 2, 3, 7, 8
- [72] Gunnar A Sigurdsson, Abhinav Gupta, Cordelia Schmid, Ali Farhadi, and Karteek Alahari. Charades-ego: A large-scale dataset of paired third and first person videos. *arXiv preprint arXiv:1804.09626*, 2018. 1, 2, 3, 6
- [73] Karen Simonyan and Andrew Zisserman. Two-stream convolutional networks for action recognition in videos. In Zoubin Ghahramani, Max Welling, Corinna Cortes, Neil D. Lawrence, and Kilian Q. Weinberger, editors, *NeurIPS*, pages 568–576, 2014. 2
- [74] Karen Simonyan and Andrew Zisserman. Very deep convolutional networks for large-scale image recognition. In Yoshua Bengio and Yann LeCun, editors, *ICLR*, 2015. 2
- [75] Bilge Soran, Ali Farhadi, and Linda Shapiro. Action recognition in the presence of one egocentric and multiple static cameras. In *ACCV*, 2014. 3
- [76] Tomáš Souček, Jean-Baptiste Alayrac, Antoine Miech, Ivan Laptev, and Josef Sivic. Look for the change: Learning object states and state-modifying actions from untrimmed web videos. In *Proceedings of the IEEE/CVF Conference on Computer Vision and Pattern Recognition (CVPR)*, pages 13956–13966, June 2022. 1
- [77] Swathikiran Sudhakaran, Sergio Escalera, and Oswald Lanz. Lsta: Long short-term attention for egocentric action recognition. In *CVPR*, 2019. 3

- [78] Christian Szegedy, Vincent Vanhoucke, Sergey Ioffe, Jonathon Shlens, and Zbigniew Wojna. Rethinking the inception architecture for computer vision. In *CVPR*, pages 2818–2826. IEEE, 2016. 2
- [79] Bugra Tekin, Federica Bogo, and Marc Pollefeys. H+ o: Unified egocentric recognition of 3d hand-object poses and interactions. In *CVPR*, 2019. 3
- [80] Aysim Toker, Qunjie Zhou, Maxim Maximov, and Laura Leal-Taixe. Coming down to earth: Satellite-to-street view synthesis for geo-localization. In *Proceedings of the IEEE/CVF Conference on Computer Vision and Pattern Recognition (CVPR)*, pages 6488–6497, June 2021. 3
- [81] Du Tran, Lubomir D. Bourdev, Rob Fergus, Lorenzo Torresani, and Manohar Paluri. Learning spatiotemporal features with 3d convolutional networks. In *ICCV*, pages 4489–4497. IEEE, 2015. 2
- [82] Du Tran, Heng Wang, Lorenzo Torresani, Jamie Ray, Yann LeCun, and Manohar Paluri. A closer look at spatiotemporal convolutions for action recognition. In *CVPR*, pages 6450–6459. IEEE, 2018. 2
- [83] Thanh-Dat Truong, Quoc-Huy Bui, Chi Nhan Duong, Han-Seok Seo, Son Lam Phung, Xin Li, and Khoa Luu. Dirrecformer: A directed attention in transformer approach to robust action recognition. In *Computer Vision and Pattern Recognition*, 2022. 2
- [84] Huiyu Wang, Mitesh Kumar Singh, and Lorenzo Torresani. Ego-only: Egocentric action detection without exocentric pretraining, 2023. 1
- [85] Limin Wang, Yuanjun Xiong, Dahua Lin, and Luc Van Gool. Untrimmednets for weakly supervised action recognition and detection. In *CVPR*, pages 6402–6411. IEEE, 2017. 1
- [86] Limin Wang, Yuanjun Xiong, Zhe Wang, Yu Qiao, Dahua Lin, Xiaoou Tang, and Luc Van Gool. Temporal segment networks: Towards good practices for deep action recognition. In Bastian Leibe, Jiri Matas, Nicu Sebe, and Max Welling, editors, *ECCV*, volume 9912, pages 20–36. Springer, 2016. 2, 8
- [87] Weiyao Wang, Du Tran, and Matt Feiszli. What makes training multi-modal classification networks hard? In *CVPR*, 2020. 3
- [88] Xiaolong Wang, Ross B. Girshick, Abhinav Gupta, and Kaiming He. Non-local neural networks. In *CVPR*, pages 7794–7803. IEEE, 2018. 2
- [89] Xiaohan Wang, Linchao Zhu, Yu Wu, and Yi Yang. Symbiotic attention for egocentric action recognition with object-centric alignment. *IEEE Transactions on Pattern Analysis and Machine Intelligence*, 2020. 3
- [90] Saining Xie, Chen Sun, Jonathan Huang, Zhuowen Tu, and Kevin Murphy. Rethinking spatiotemporal feature learning: Speed-accuracy trade-offs in video classification. In Vittorio Ferrari, Martial Hebert, Cristian Sminchisescu, and Yair Weiss, editors, *ECCV*, volume 11219, pages 318–335. Springer, 2018. 2
- [91] Mingze Xu, Chenyou Fan, Yuchen Wang, Michael S Ryoo, and David J Crandall. Joint person segmentation and identification in synchronized first-and third-person videos. In *ECCV*, 2018. 3
- [92] Liang Yang, Hao Jiang, Jizhong Xiao, and Zhouyuan Huo. Ego-downward and ambient video based person location association. *arXiv preprint arXiv:1812.00477*, 2018. 3
- [93] Bolei Zhou, Alex Andonian, Aude Oliva, and Antonio Torralba. Temporal relational reasoning in videos. In Vittorio Ferrari, Martial Hebert, Cristian Sminchisescu, and Yair Weiss, editors, *ECCV*, volume 11205 of *Lecture Notes in Computer Science*, pages 831–846. Springer, 2018. 2, 8
- [94] Sijie Zhu, Mubarak Shah, and Chen Chen. Transgeo: Transformer is all you need for cross-view image geo-localization. In *Proceedings of the IEEE/CVF Conference on Computer Vision and Pattern Recognition*, pages 1162–1171, 2022. 3



## Proof of Eqn (9)

$\mathcal{D}_x$  and  $\mathcal{D}_a$  are the metrics that measure the correlation of videos and attention maps, respectively; therefore, for all  $\mathbf{x}_{ego}$  and  $\mathbf{a}_{ego}$ , these metrics have to satisfy the triangular inequality as follows:

$$\begin{aligned}\mathcal{D}_x(\mathbf{x}_{exo}, \mathbf{x}_{ego}) + \mathcal{D}_x(\mathbf{x}_{ego}, \bar{\mathbf{x}}_{ego}) &\geq \mathcal{D}_x(\mathbf{x}_{exo}, \bar{\mathbf{x}}_{ego}) \\ \mathcal{D}_a(\mathbf{a}_{exo}, \mathbf{a}_{ego}) + \mathcal{D}_a(\mathbf{a}_{ego}, \bar{\mathbf{a}}_{ego}) &\geq \mathcal{D}_a(\mathbf{a}_{exo}, \bar{\mathbf{a}}_{ego})\end{aligned}\tag{12}$$

In addition, under our cross-view distribution shift assumption, the metrics  $\mathcal{D}_x$  and  $\mathcal{D}_a$  are bounded by a threshold  $\beta$ , i.e.,  $\mathcal{D}_x(\mathbf{x}_{exo}, \mathbf{x}_{ego}) \leq \beta$  and  $\mathcal{D}_a(\mathbf{a}_{exo}, \mathbf{a}_{ego}) \leq \beta$ . As a result, the cross-view self-attention constraint can be further extended as follows:

$$\begin{aligned}&\mathcal{D}_x(\mathbf{x}_{exo}, \bar{\mathbf{x}}_{ego}) - \alpha \mathcal{D}_a(\mathbf{a}_{exo}, \bar{\mathbf{a}}_{ego}) \\ &\leq \mathcal{D}_x(\mathbf{x}_{exo}, \mathbf{x}_{ego}) + \mathcal{D}_x(\mathbf{x}_{ego}, \bar{\mathbf{x}}_{ego}) - \alpha \mathcal{D}_a(\mathbf{a}_{exo}, \bar{\mathbf{a}}_{ego}) \\ &\leq \mathcal{D}_x(\mathbf{x}_{exo}, \mathbf{x}_{ego}) + \beta - \alpha(\mathcal{D}_a(\mathbf{a}_{exo}, \mathbf{a}_{ego}) + \beta) + \alpha\beta \\ &\leq \mathcal{D}_x(\mathbf{x}_{exo}, \mathbf{x}_{ego}) - \alpha \mathcal{D}_a(\mathbf{a}_{exo}, \mathbf{a}_{ego}) + (1 + \alpha)\beta\end{aligned}\tag{13}$$